

# Application of the trickle tower to problems of pollution control.

## III. Heavy-metal cyanide solutions

E. A. EL-GHAOUI<sup>†</sup>, R. E. W. JANSSON

Chemistry Department, Southampton University, Southampton, UK

Received 18 February 1981

The destruction of  $\text{CN}^-$  and co-deposition of copper, cadmium, nickel, zinc and lead, both as simple solutions and as mixtures, have been investigated in a number of trickle towers with from 8 to 49 layers of cells. Specific chemical effects due to the formation of cyano-complexes of some of the metals are evident, and it has been found that copper, nickel and cadmium accelerate the destruction of  $\text{CN}^-$ , at least initially. For simple solutions a previously proposed scaling law is adequate.

### Nomenclature

$a$	length of bipolar element (cm)
$c$	concentration (ppm)
$c^0$	initial concentration (ppm)
$K$	mass transfer coefficient ( $\text{cm s}^{-1}$ )
$K' = K\theta_L$	effective mass transfer coefficient ( $\text{cm s}^{-1}$ )
$L$	wetted perimeter per layer of packing (cm)
$p$	number of layers of cells
$t$	time (s)
$v_o$	volumetric flow rate ( $\text{cm}^3 \text{s}^{-1}$ )
$V$	inventory of solution ( $\text{cm}^3$ )
$\theta_L$	fractional active length
$\phi_s^R$	reversible potential with respect to main counter reaction (V)
$\phi_s^T$	potential applied across an element with respect to main counter reaction (V)

### 1. Introduction

Parts I and II of this series dealt with the scavenging of metal ions from dilute acid solutions [1] and the direct and indirect destruction of cyanide in dilute alkaline streams [2]. A very common kind of industrial effluent consists of a dilute solution of heavy-metal cyanides, e.g., plating-bath wash water, so that both the cation and anion have been removed. Since the destruction of  $\text{CN}^-$  by

electrogenerated hypochlorite was so much faster than its direct oxidation [2], chloride was added to all the systems reported here. In some cases, however, the metal itself accelerated the rate of  $\text{CN}^-$  removal to such an extent that this may not always be necessary. The characteristics and operations of the trickle tower have been fully described elsewhere [1, 2]. The chemical systems studied were single solutions of  $\text{Cu}^{2+}$ ,  $\text{Ni}^{2+}$ ,  $\text{Cd}^{2+}$ ,  $\text{Pb}^{2+}$  and  $\text{Zn}^{2+}$ , all with excess  $\text{CN}^-$ , and mixtures of these solutions.

It has been shown that the overpotential rises so rapidly towards the end of an element in a trickle tower that reactions are effectively mass-transfer controlled [3]. Under these conditions and in batch recycling the decrease in concentration in the reservoir can be expressed by

$$-\ln \frac{c}{c^0} = \frac{v_o}{V} \left[ 1 - \exp \left( -\frac{K\theta_L a L p}{v_o} \right) \right] t. \quad (1)$$

The parameter  $\theta_L$  is the fraction of the length of an element which is active, and can be calculated [1] for well-defined cathodic and anodic reactions. However, in the systems described here a number of reactions can take place and it will be shown below that during one depletion run the mechanism may change more than once so that it is difficult to calculate  $\theta_L$  *ab initio*. By rearrangement, Equation 1 gives

<sup>†</sup> Present address: Chemistry Department, Lebanese University, Hadeth, Beirut, Lebanon.

$$-K' = -K\theta_L = \frac{v_o}{aLp} \ln \left[ 1 + \frac{V}{v_o} \frac{1}{t} \ln \frac{c}{c^0} \right] \quad (2)$$

where  $K'$  is an effective mass-transport coefficient, which can be determined from the experimental data. By using measured values of  $K$  from simpler systems [1] estimates of  $\theta_L$  can be made.

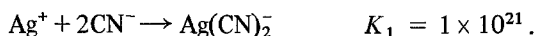
Equation 1 can then be used as the design equation for a tower to perform any given duty.

## 2. Experimental

Two towers were used; a small one of 62 mm internal diameter packed with seven layers of 6.5 mm × 6.5 mm graphite Raschig rings (total wetted perimeter of 242 cm per layer) and a long one of 75 mm internal diameter packed with 20, 34 or 48 layers of 12.5 mm × 12.5 mm rings (total wetted perimeter 181 cm per layer). Together with the feeder electrodes this gave  $(n + 1)$  cells in series for  $n$  layers of packing. Experiments were run with batch recycling, samples being taken at intervals for analysis. Usually the solutions initially contained 100 ppm of the metal, 300 ppm of  $\text{CN}^-$  and 0.135 mol  $\text{dm}^{-3}$  NaCl, the pH being adjusted to about 10 [2]. In early experiments with the short tower, the applied voltage was 2.25 V per layer, but this was reduced to 2.0 V per layer in the large tower.

For comparison purposes, some experiments were run in a 51 mm × 12.5 mm × 230 mm flow-by packed-bed electrode of graphite granules [4]; anode and cathode compartments were separated by a Nafion membrane. The applied potential was 2.5 V.

Metal-ion concentrations were estimated with a Varian Techtron (model 1100) atomic absorption spectrometer. Cyanide was estimated by Liebig's method [5, 6, 7] which depends on the formation of a soluble complex of  $\text{Ag}^+$  as long as there is excess  $\text{CN}^-$ ;



At the equivalence point, the addition of further  $\text{Ag}^+$  causes the precipitation of insoluble  $\text{AgCN}$



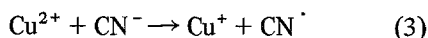
In the presence of heavy metals which can also form cyano-complexes, the question arises whether Liebig's method is capable of estimating the total

cyanide present. However, stability constants show [8] that only  $[\text{Ni}(\text{CN})_4]^{2-}$  is more stable than  $\text{Ag}(\text{CN})_2^-$  and trial determinations on made-up, known solutions showed that the cyanide could be estimated in  $\text{Ni}^{2+}/\text{CN}^-$  solutions with better than 7% accuracy. Since in these experiments chloride was present in massive excess it is likely that  $\text{Ag}^+$  was able to displace  $\text{CN}^-$  from the nickel complex through the formation of substitution complexes  $\text{Ni}(\text{CN})_3\text{Cl}^{2-}$ ,  $\text{Ni}(\text{CN})_2\text{Cl}_2^-$  etc. and therefore what was estimated was close to being the total cyanide present.

## 3. Results and discussion

### 3.1. Small tower

Fig. 1 shows concentration-time curves for batch depletion of  $\text{CN}^-$  in the presence of heavy metals compared with data [2] for its direct and indirect oxidation. It can be seen that, relative to the rate of indirect oxidation in the absence of heavy metals,  $\text{Pb}^{2+}$  and  $\text{Zn}^{2+}$  retard the rate but  $\text{Cu}^{2+}$ ,  $\text{Ni}^{2+}$  and  $\text{Cd}^{2+}$  all substantially accelerate it, at least initially. A very rapid decrease in  $\text{CN}^-$  concentration was found on adding  $\text{Cu}^{2+}$  to a sodium cyanide solution due to the reaction



so that the initial concentration of  $\text{CN}^-$  was about 200 ppm in this case, but even thereafter the rate remained high. Plots of  $\ln c/c^0$  versus time were linear, according to Equation 1, but, in the presence of  $\text{Cu}^+$ ,  $\text{Ni}^{2+}$  and  $\text{Cd}^{2+}$ , part way through each run a definite change in mechanism was indicated by a change in slope (see, e.g., Fig. 2).

Only in the case of  $\text{Pb}^{2+}$  did the metal deposit from  $t = 0$  (Fig. 2); in other cases the deposition was delayed until a critical value of  $(\text{CN}^-)/(\text{M}^{n+})$  was attained. Because of the shapes of the curves it is hard to detect the onset of deposition accurately, but approximate values of the ratio  $(\text{CN}^-)/(\text{M}^{n+})$  are:

Metal ion:	$\text{Cu}^+$	$\text{Ni}^{2+}$	$\text{Cd}^{2+}$	$\text{Zn}^{2+}$
Ratio:	1.2	2.8	~ 6	5.1.

Remembering that  $\text{Cl}^-$  can substitute for  $\text{CN}^-$  in heavy-metal complexes, clearly these numbers are consistent with the stoichiometry of known cyano-

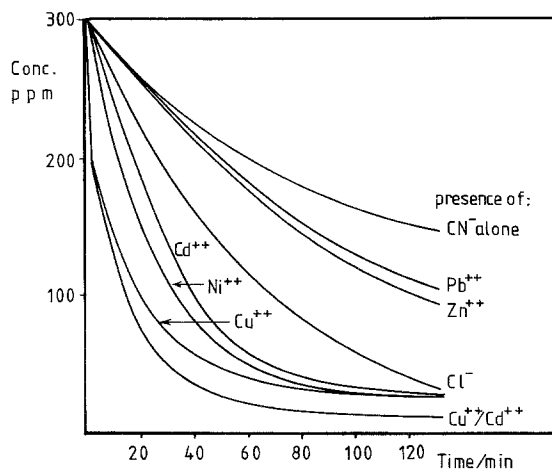


Fig. 1. Oxidation of cyanide in the presence of heavy metals. Small trickle tower, 2.25 V/layer,  $0.6 \text{ dm}^3 \text{ min}^{-1}$ .

complexes [9] or the preferred co-ordination of the ion in solution. Interestingly the abrupt change in slope for  $\text{Cd}^{2+}$  takes place with a ratio very close to three.

Using Equation 2 an estimate of the fractional active length  $\theta_L$  for each system was obtained from the slope of the semilog plot and previously determined mass-transfer data [1] interpolated at the appropriate value of  $(v_o/L)$ , i.e.  $uh$ . Some results are shown in Table 1.

In general the destruction of  $\text{CN}^-$  in the presence of mixtures of cations is faster than the presence of a single cation (e.g. the curve for  $\text{Cu}^+/\text{Cd}^{2+}$  in Fig. 1) and the rate of metal deposition is greater; again complexation is important.

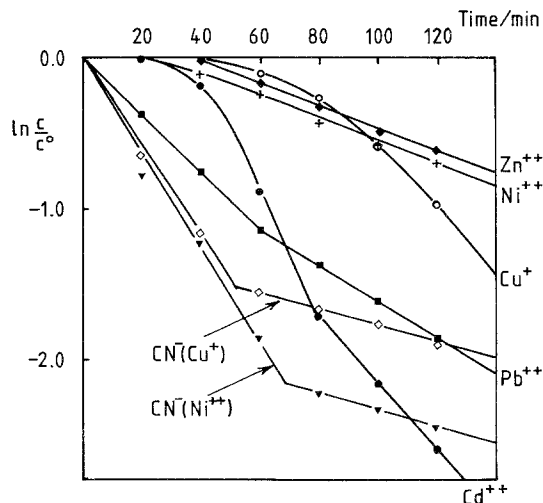


Fig. 2. Deposition of metals during oxidation of cyanide. Small trickle tower, 2.25 V/layer,  $0.6 \text{ dm}^3 \text{ min}^{-1}$ .

This can be seen from Fig. 3; in the binary mixture  $\text{Cu}^+/\text{Cd}^{2+}$  the deposition of metal is clearly delayed until the  $\text{CN}^-$  has fallen to a low value, but when  $\text{Ni}^{2+}$  is added to a mixture metal deposition begins immediately although the rate of removal of cyanide is very slightly less. Significantly all the metals are deposited, not just the one with the least stable complex, and despite their differences in reversible potential. Estimates of  $K'$  and  $\theta_L$  for mixed systems are also given in Table 1. The deposition rates in a  $\text{Pb}^{2+}/\text{Zn}^{2+}/\text{CN}^-$  mixture are similar to those in the simple  $\text{M}^{2+}/\text{CN}^-$  solutions.

Table 1. Effective rate constant  $K'$  ( $\text{cm s}^{-1}$ ) and fractional active area  $\theta_L$  in small trickle tower

Metal ion	Anodic reaction				Cathodic reaction	
	From initial $\text{CN}^-$ rate		From final $\text{CN}^-$ rate		From final $\text{M}^{n+}$ rate	
	$10^4 K'$	$\theta_L$	$10^4 K'$	$\theta_L$	$10^4 K'$	$\theta_L$
$\text{Cu}^+$	4.0	0.65	0.7	0.12	2.7	0.44
$\text{Ni}^{2+}$	4.3	0.69	0.7	0.12	1.1	0.17
$\text{Cd}^{2+}$	3.9	0.63	1.4	0.22	3.0	0.48
$\text{Zn}^{2+}$	1.2	0.20	1.2	0.20	1.0	0.16
$\text{Pb}^{2+}$	1.2	0.19	1.2	0.19	1.6	0.25
$\text{Cu}^+/\text{Cd}^{2+}$	5.4	0.87	1.8	0.29	2.8	0.46 (Cu)
					1.4	0.23 (Cd)
$\text{Cu}^+/\text{Cd}^{2+}/\text{Ni}^{2+}$	4.9	0.79	2.5	0.41	2.3	0.37 (Cu)
					2.6	0.41 (Cd)
					2.2	0.35 (Ni)

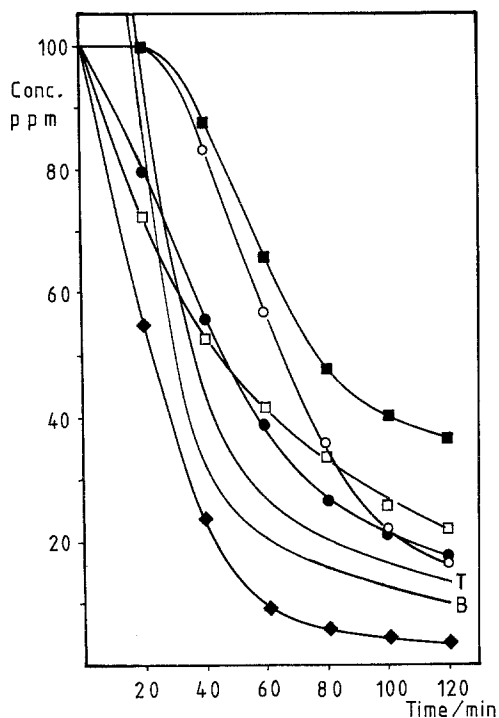


Fig. 3. Oxidation of cyanide and deposition of metals from mixtures. Small trickle tower, 2.25 V/layer,  $0.6 \text{ dm}^3 \text{ min}^{-1}$ . B,  $\text{CN}^-$  in binary  $\text{Cu}^+/\text{Cd}^{2+}$  mixture; ■,  $\text{Cd}^{2+}$  in binary  $\text{Cu}^+/\text{Cd}^{2+}$  mixture; ○,  $\text{Cu}^+$  in binary  $\text{Cu}^+/\text{Cd}^{2+}$  mixture. T,  $\text{CN}^-$  in ternary  $\text{Cu}^+/\text{Cd}^{2+}$  mixture; □,  $\text{Ni}^{2+}$  in ternary  $\text{Cu}^+/\text{Cd}^{2+}/\text{Ni}^{2+}$  mixture; ●,  $\text{Cd}^{2+}$  in ternary  $\text{Cu}^+/\text{Cd}^{2+}/\text{Ni}^{2+}$  mixture; ◆,  $\text{Cu}^+$  in ternary  $\text{Cu}^+/\text{Cd}^{2+}/\text{Ni}^{2+}$  mixture.

### 3.2. Large tower

As expected, the rate of removal of both  $\text{CN}^-$  and  $\text{M}^{2+}$  increase with the length of the tower. As an

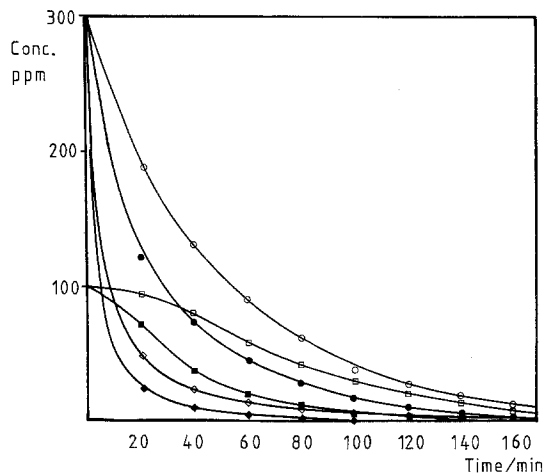


Fig. 4. Oxidation of cyanide and deposition of copper in the large trickle tower. 2 V layer,  $1.5 \text{ dm}^3 \text{ min}^{-1}$ . ○, 21 layers,  $\text{CN}^-$  in absence of copper; ◇, 21 layers,  $\text{CN}^-$  in presence of  $\text{Cu}^+$ ; □, 21 layers,  $\text{Cu}^+$ ; ●, 49 layers,  $\text{CN}^-$  in absence of copper; ◆, 49 layers,  $\text{CN}^-$  in presence of  $\text{Cu}^+$ ; ■, 49 layers,  $\text{Cu}^+$ .

example, Fig. 4 shows that cyanide is removed so rapidly that there is virtually no delay in the removal of copper with 21 layers of cells, and that with 49 layers 90% depletion of  $\text{CN}^-$  is obtained in 10 or 12 recycles of the inventory of solution. The difference between the rate in the presence and absence of  $\text{Cu}^+$  is also shown. Similar results are obtained with nickel and cadmium solutions. At early batch times (high concentrations) the current efficiency is typically 80%, but naturally this falls to about 10% at terminal concentrations.

Table 2. Effective rate constant  $K'$  ( $\text{cm s}^{-1}$ ) and fractional active area  $\theta_L$  in large trickle towers

Systems	Number of layers					
	21		35		49	
	$10^4 K'$	$\theta_L$	$10^4 K'$	$\theta_L$	$10^4 K'$	$\theta_L$
Cu	1.5	0.18	2.6	0.30	2.5	0.29
$\text{CN}^-$ , initial	6.0	0.70	6.6	0.76	6.5	0.76
$\text{CN}^-$ , final	1.6	0.18	1.6	0.19	1.2	0.14
Cd	1.6	0.18	1.9	0.22	2.2	0.26
$\text{CN}^-$ , initial	3.0	0.35	2.6	0.30	2.4	0.28
$\text{CN}^-$ , final	1.7	0.19	1.3	0.15	1.1	0.13
Ni	0.5	0.06	0.5	0.05	0.4	0.04
$\text{CN}^-$ , initial	5.0	0.56	5.5	0.64	3.2	0.37
$\text{CN}^-$ , final	1.6	0.19	1.3	0.16	1.0	0.11

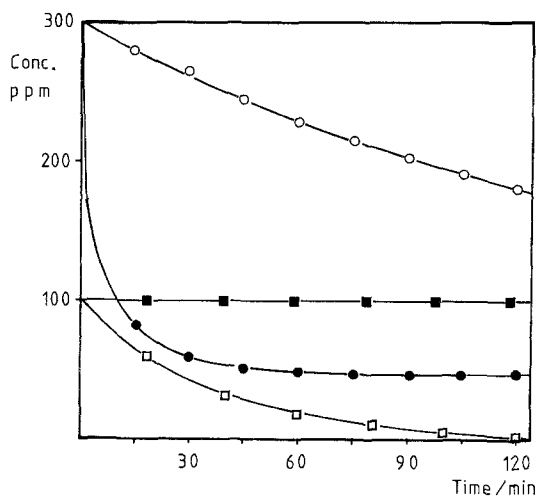


Fig. 5. Oxidation of cyanide and deposition of copper in monopolar packed beds; Anodic bed:  $\circ$ ,  $\text{CN}^-$  in absence of copper;  $\bullet$ ,  $\text{CN}^-$  in presence of  $\text{Cu}^+$ . Cathodic bed:  $\square$ ,  $\text{Cu}^{2+}$  in absence of  $\text{CN}^-$ ;  $\blacksquare$ ,  $\text{Cu}^+$  in presence of  $\text{CN}^-$ .

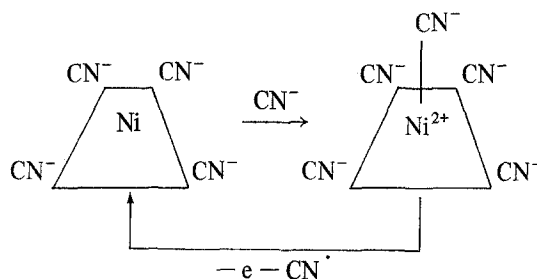
As the conversion per pass can be as high as 50% with the longest tower there may be a considerable variation in stoichiometry between the top and the bottom of the column, with different mechanisms controlling the destruction of  $\text{CN}^-$  and removal of  $\text{M}^{n+}$ . Nevertheless it is still possible to apply Equation 2 and the results are shown in Table 2.

### 3.3. Packed bed

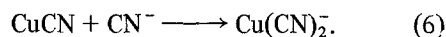
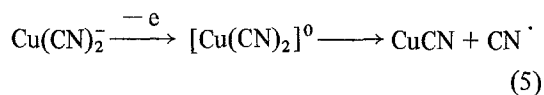
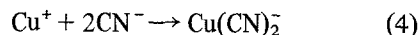
Fig. 5 shows the results of depletion experiments in cathodic and anodic packed beds. In the anodic bed  $\text{CN}^-$  is oxidized much more rapidly in the presence of  $\text{Cu}^+$  than in its absence but a limiting stoichiometry is reached of  $[\text{Cu}^+]/[\text{CN}^-] = 1.05$ , whereas in the cathodic bed, copper could not be deposited at all from a cyanide solution at an applied potential of 2.5 V. It is significant that copper is first deposited in the trickle tower when  $[\text{Cu}^+]/[\text{CN}^-]$  is of the order of unity, as shown above.

## 4. General discussion

Bishop [10] has suggested that Ni(II) accelerates the rate of  $\text{CN}^-$  oxidation through the formation of easily oxidizable complexes, e.g.



until all the excess  $\text{CN}^-$  has been consumed. Similar considerations probably apply in the cases of copper and cadmium, e.g.



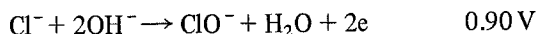
Now the fractional active length of a ring is approximately given by [1]

$$\theta_L = 1 - \left( \frac{\phi_s^R}{\phi_s^T} \right) \quad (7)$$

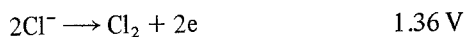
where  $\phi_s^T$  is the potential applied across one element of packing and  $\phi_s^R$  is the reversible potential of the (in this case anodic) reaction, both with respect to the principal counter reaction. Before the onset of metal deposition the counter reaction must be hydrogen evolution, so  $\phi_s^R$  depends almost exclusively on the anodic reaction and if the oxidation of the complex is more facile than the oxidation of  $\text{Cl}^-$  not only will it be preferred to  $\text{Cl}_2$  evolution as a means of destroying  $\text{CN}^-$  but  $\theta_L$  will be large. This explains why it is possible for the overall rate to increase in the presence of some metals (Tables 1 and 2) even though the system remains mass-transport controlled; activation controls the effective area even though it does not control the rate itself. For those metals forming cyano-complexes in solution, when the  $\text{CN}^-$  concentration has fallen to the stoichiometry of the lowest stable complex then metal deposition commences. In the cases of copper, cadmium and nickel solutions, soon after this but before the limiting rate has been attained the rate of  $\text{CN}^-$  removal also changes (Fig. 2). This is understandable since the absence of an easily oxidizable cyano-complex raises  $\phi_s^R$  to that for  $\text{Cl}^-$  or  $\text{CN}^-$

oxidation, thereby diminishing the anodic active area, hence the rate.

In the case of zinc and lead single solutions, the low rate for  $\text{CN}^-$  oxidation is probably due to the high reversible potentials for metal deposition and the high overpotential for hydrogen evolution on both these metals; since  $\phi_s^R$  is high for the anodic reaction (with respect to the cathodic counter reactions)  $\phi_s^R/\phi_s^T$  is large, therefore  $\theta_L$  small and the effective rate low. Likewise the change in lead deposition rate (Fig. 2) is probably due to the falling pH changing the anodic reaction from



to



thus making ( $\phi_s^R$ ) for the cathodic reaction larger, hence the cathodic  $\theta_L$  smaller. The synergism between the anodic and cathodic reactions is striking.

As Fig. 5 shows, it is interesting that  $[\text{CN}^-]$  may quickly be reduced in an anodic bed electrode *via* a scheme such as Reactions 4, 5 and 6, but that the concentration can not be lowered below  $[\text{Cu}^+]/[\text{CN}^-] = 1$ , at least under the conditions of the present experiments. Similarly, in a cathodic bed, copper could not be deposited as long as cyanide was in excess, but both the cyanide and copper concentrations could be lowered continuously in the trickle tower since the solution was exposed to both anodes and cathodes; during this process the stoichiometry continually changed. On the grounds of active area the rate of removal in the packed bed should have been three times higher than the rate in the small trickle tower, whereas the rate in the trickle tower was in fact,

5.3 times the rate in the packed bed. The alternation of polarity is clearly important.

In the case of metal mixtures the behaviour is very complicated, but the role of complexation is again evident. For example (Fig. 4), initially there is enough  $\text{CN}^-$  to complex all the  $\text{Cu}^+$  and  $\text{Cd}^{2+}$  in the binary mixture and the 'normal' delay in metal deposition is observed. However, in the ternary mixture with  $\text{Ni}^{2+}$  all three components are at about their 'critical ratios' initially and deposition is immediate. With such specific chemical effects and because conditions change with position within a single long tower the use of Equation 1 as a general scaling law is dubious in these cases, but it is clear that, because of its unique contacting pattern, the trickle tower is capable of dealing effectively and largely self-adaptively with a number of difficult effluents.

## References

- [1] S. Ehdai, M. Fleischmann and R. E. W. Jansson, *J. Appl. Electrochem.* **12** (1982) 59.
- [2] E. A. El-Ghaoui, R. E. W. Jansson and C. Moreland, *ibid.* **12** (1982) 69.
- [3] M. Fleischmann and R. E. W. Jansson, *Chem. Ingnr. Techn.* **49**(4) (1977) 283.
- [4] F. Sarfarazi, PhD thesis, Southampton University (1979).
- [5] N. Furman, 'Standard Methods for Chemical Analysis', Vol. 1, 6th edn, van Nostrand Inc., New York (1962).
- [6] F. Fludzak, *Anal. Chem.* **26** (1953) 1784.
- [7] J. Waser, 'Quantitative Chemistry', Benjamin Inc., New York (1964).
- [8] J. Kleinberg, W. Argersinger and E. Griscolod, 'Inorganic Chemistry', D. Heath, New York (1960).
- [9] T. Moeller, 'Inorganic Chemistry; An Advanced Textbook', Chapman and Hall Ltd, London (1958).
- [10] E. Bishop, *Meeting of the Electrochemical Society, City University, London, May 1975.*